Combined Density Functional Theory and Molecular Mechanics (QM/MM) Study of Single-Site Ethylene Polymerization and Chain Termination for the Catalysts $[(C_6R_5N{=}CH)C_4H_3N]_2PrTi^+$ (R = F, H) and [bis(η^5-1-indenyl)dimethylsilane]$PrZr^+$ in the Presence of the Counterion $CH_3B(C_6F_5)_3^-$

Kumar Vanka, Zhitao Xu, and Tom Ziegler*

Department of Chemistry, University of Calgary, Calgary, Alberta, Canada T2N 1N4

Received September 14, 2004

Calculations, using density functional theory, have been carried out to investigate two chain termination processes, (i) unimolecular hydrogen transfer to the metal center and (ii) bimolecular hydrogen transfer to the incoming ethylene monomer, for the PI systems $[(C_6R_5N{=}CH)C_4H_3N]_2PrTi$-$\mu$-$CH_3$-$B(C_6F_5)_3$ (R = F, H). A validated QM/MM model was used to represent the counterion. The barriers for the unimolecular termination process were about 36.5 kcal/mol for both the PI systems studied, while the rate-determining uptake barriers for the bimolecular chain termination process were about 18 kcal/mol lower for both PI systems. A difference of only about 0.5 kcal/mol was observed between the corresponding barriers for each of the termination processes for the two systems. The insertion of the ethylene monomer into the Ti−C bond was also investigated for the two PI systems, and the rate-determining uptake barrier was found to be about 6 kcal/mol lower than the corresponding rate-determining uptake barriers for bimolecular termination. The effect of increasing the steric bulk on the phenyl groups attached to the imine nitrogen was investigated for the $[(C_6R_5N{=}CH)C_4H_3N]_2PrTi$-$\mu$-$CH_3$-$B(C_6F_5)_3$, with the hydrogen at the ortho position of the phenyl rings being replaced by tertiary butyl groups, modeled by MM atoms. The rate-determining uptake barrier for the bimolecular chain termination process for this system was found to be only marginally higher than the corresponding uptake barrier for the non-bulky system. Insertion and uni- and bimolecular termination processes were also investigated for the *ansa*-indenyl system [bis(η^5-1-indenyl)dimethylsilane]ZrPr-μ-Me-$B(C_6F_5)_3$. The barriers for insertion and bimolecular chain termination for this system were comparable to those for the PI systems, but the barrier to unimolecular chain termination was found to be about 5 kcal/mol higher.

I. Introduction

The field of olefin polymerization by single-site homogeneous catalysts has seen remarkable growth and development over the past 20 years.[1] The ability of single-site catalysts to achieve high stereoselectivity and narrow molecular weight distribution has made them emerge as viable alternatives to traditional Ziegler−Natta type heterogeneous catalysts.[2] The fact that they are structurally well-defined active mononuclear complexes has allowed the systematic modification of their structures for enhanced control over polymer properties. The state-of-the-art homogeneous catalysts transform simple alkenes into polymers with rate accelerations and stereo- and regiospecificities that rival those of enzymatic catalysts.

Among the more highly active homogeneous catalysts are metallocenes and related organometallic compounds containing a group IV transition metal. The general structure of these complexes consists of a group 4 transition-metal center (M) coordinated to two ligands (L) and two methyl groups: L_2MMe_2. Bis(cyclopentadienyl) (bis-Cp) complexes of the early transition metals are highly effective homogeneous olefin polymerization catalysts, but extensive patent coverage has spurred the development of new catalysts that do not contain the bis-Cp ligand framework.[3] Recently Yoshida et al.[4a] have prepared titanium complexes with two pyrrolide−imine chelate ligands (henceforth referred to as the PI system), $[(C_6H_5N{=}CH)C_4H_3N]_2TiCl_2$ (see Figure 1), which upon activation by MAO produced active polymerization

(1) (a) Resconi, L.; Cavallo, L.; Fait, A.; Piemontesi, F. *Chem. Rev.* **2000**, *100*, 1253. (b) Mashima, K.; Nakayama, Y.; Nakamura, A. *Adv. Polym. Sci.* **1997**, *133*, 1. (c) Alt, H. G.; Koppl, A. *Chem. Rev.* **2000**, *100*, 1205.

(2) *Metallocene-Catalyzed Polymers: Materials, Properties, Processing and Markets*; Benedikt, G. M., Goodall, B. L., Eds.; Plastic Design Library: New York, 1998.

(3) (a) Britovsek, G. P.; Gibson, V. C.; Waas, D. F. *Angew. Chem., Int. Ed.* **1999**, *38*, *429.* (b) Liang, L.-C.; Schrock, R. R.; Davis, W. M.; McConville, D. H. *J. Am. Chem. Soc.* **1999**, *121*, 5797. (c) Baumann, R.; Stumpf, R.; Davis, W. M.; Liang, l.-C.; Schrock, R. R. *J. Am. Chem. Soc.* **1999**, *121*, 7822. (d) Guerin, F.; Stewart, J. C.; Beddie, C.; Stephan, D. W.; *Organometallics* **2000**, *19*, 2994. (e) Yue, N.*;* Hollink, E.; Guerin, F.; Stephan, D. W. *Organometallics* **2001***, 20*, 4424.

10.1021/om0492808 CCC: $30.25
Publication on Web 01/04/2005

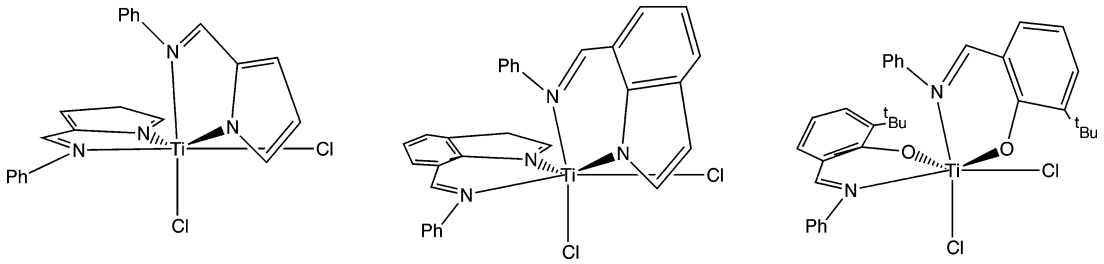

Figure 1. Structures of post-metallocene catalyst systems having more than two ancillary ligands attached to them.

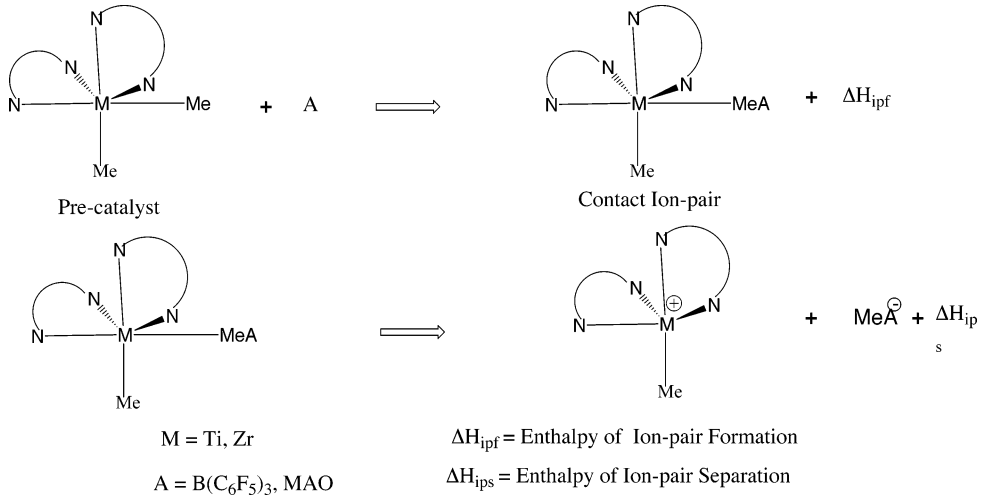

Figure 2. Mechanism for the ion pair formation and separation in the octahedral contact ion pair systems.

catalysts. A modified version of these catalyst systems,[4e] having phenoxy−imine ligands attached to the nitrogen (FI systems), [7-(RN=CH)C_8H_5N]$_2TiCl_2$ (R = phenyl and phenyl derivatives), exhibit the characteristics of living ethylene polymerization. Other catalysts, also showing high activities, that have been prepared[4d] have indolide−imine chelating ligands attached to the titanium (see Figure 1).

The complexes shown in Figure 1 can be converted to polymerization catalysts with the help of a cocatalyst. The process of activation is depicted in Figure 2. First, a methyl group is extracted by the acidic cocatalyst compound, denoted as A in the figure. This leads to a charge-separated contact ion pair. The formation of this ion-pair species is exothermic, with the enthalpy of ion-pair formation denoted as ΔH_{ipf} in Figure 2. The ion pair can then separate into the active catalyst species and the anion, MeA^-. The energy required for a complete separation is denoted as ΔH_{ips}. Experimental and computational evidence indicates ΔH_{ips} to be very high,[5] and so the counterion MeA^- is likely to stay in the vicinity of the cation during the polymerization process, in the form of a contact ion pair.

The contact ion pair thus formed can then act as the site for the olefin polymerization. The generally accepted mechanism for the insertion of the monomer is the Cossee−Arlman mechanism, shown in Figure 3 for the PI system. First, the monomer (ethylene, in Figure 2) approaches the contact ion pair and binds to it, forming a weak olefin complex. The enthalpy of this complexation is denoted as ΔH_c. From this complexed state, the ethylene monomer then approaches the alkyl chain and attempts to insert into the metal−alkyl bond, leading to a four-centered transition state. The internal barrier of the reaction path, from the olefin complex to the transition state, is defined as ΔH_{ib}. The total barrier of the reaction is denoted as ΔH_{tot} and is the sum of ΔH_c and ΔH_{ib}.

During the polymerization process, alongside the insertion at the catalyst center, side reactions can also take place, leading to termination of the polymer chain. The two principal ways in which the catalyst can terminate are (i) through transfer of a hydrogen from the β-carbon of the chain onto the incoming monomer, a process which is bimolecular and dependent on the concentrations of the catalyst and the monomer, and (ii) through transfer of a hydrogen from the carbon of the chain to the metal center in the absence of the monomer, a unimolecular process independent of monomer concentration. Both of these processes are detailed in Figure 4, for the ethylene monomer and the PI catalyst. Experimental evidence exists[6] for chain termination by either of these two mechanisms.

There have been several theoretical studies conducted on the insertion and the termination[7] processes for naked cationic catalyst systems. However, due to the

(4) (a) Yoshida, Y.; Matsui, S.; Takagi, Y.; Mitani, M.; Nitabaru, M.; Nakano, T.; Tanaka, H.; Fujita, T. *Chem. Lett.* **2000**, 1270. (b) Yoshida, Y.; Matsui, S.; Takagi, Y.; Mitani, M.; Nakano, T.; Tanaka, H.; Kashiwa, N.; Fujita, T. *Organometallics* **2001**, *20*, 4793. (c) Matsui, S.; Mitani, M.; Saito, J.; Tohi, Y.; Makio, H.; Matsukawa, N.; Takagi, Y.; Tsuru, K.; Nitabaru, M.; Nakano, T.; Tanaka, H.; Kasjiwa, N.; Fujita, T. *J. Am. Chem. Soc.* **2001**, *123*, 6387. (d) Matsugi, T.; Matsui, S.; Kojoh, S.; Takagi, Y.; Inoue, Y.; Nakano, T.; Fujita, T.; Kashiwa, N. *Macromolecules* **2002**, *35*, 4880. (e) Mitani, M.; Mohri, J.; Yoshida, Y.; Saito, J.; Ishii, S.; Tsuru, K.; Matsui, S.; Furuyama, R.; Nakano, T.; Tanaka, H.; Kojoh, S.; Matsugi, T.; Kashiwa, N.; Fujita, T. *J. Am. Chem.* Soc. **2002**, *124*, *3327*. (f) Reinartz, S.; Mason, A. F.; Lobkovsky, E. B.; Coates, G. W. *Organometallics* **2003**, *22*, 2542.

(5) (a) Yang, X.; Stern, C. L.; Marks, T. J. *J. Am. Chem. Soc.* **1994**, *116*, 10015. (b) Deck, P. A.; Marks, T. J. *J. Am. Chem. Soc.* **1995**, *117*, 6128. (c) Jia, L.; Stern, C. L.; Marks, T. J. *Organometallics* **1997**, *16*, 842. (d) Li, L.; Marks, T. J. *Organometallics* **1998**, *17*, 3996. (e) Chan, M. S. W.; Ziegler, T. *Organometallics* **2000**, *19*, 5182.

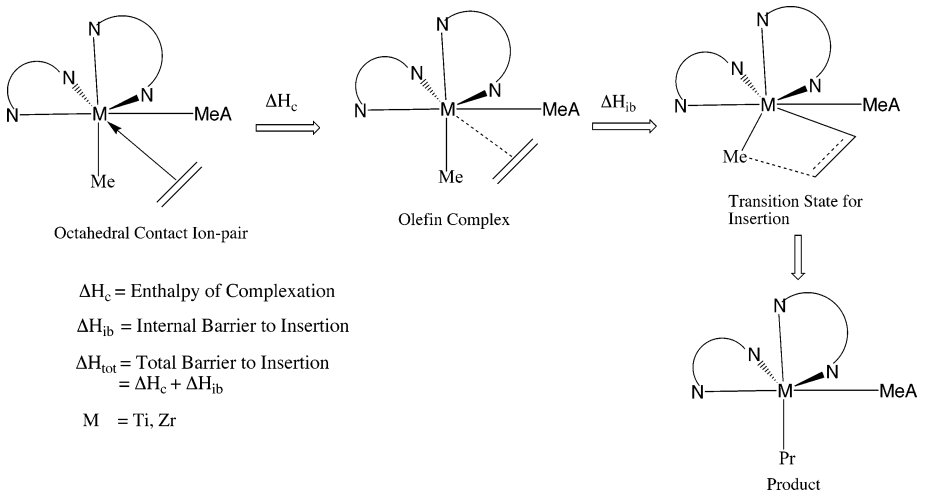

Figure 3. Mechanism for ethylene monomer approach, complexation, and insertion into the M−Me bond.

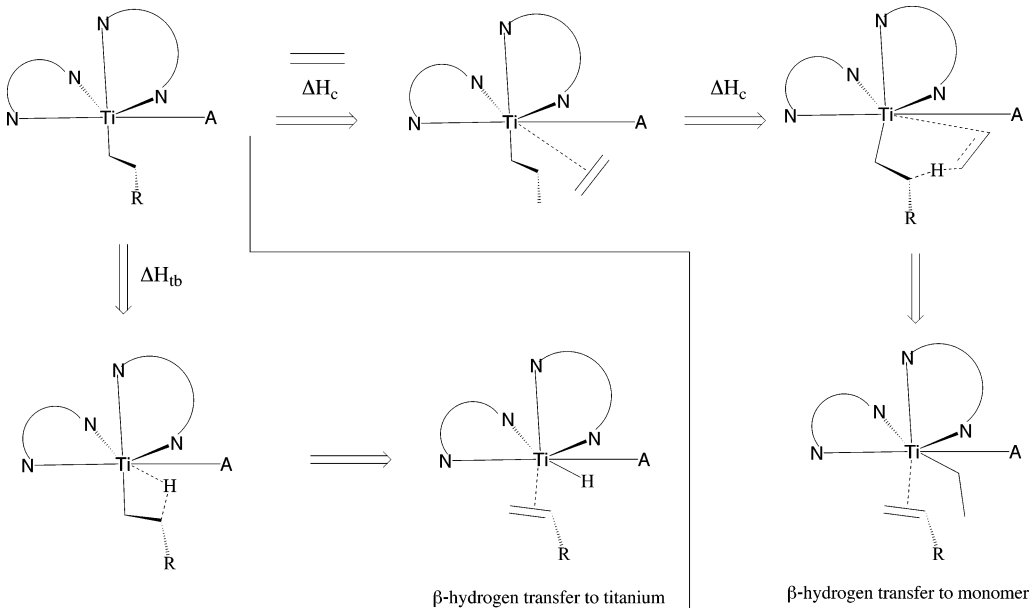

Figure 4. Different pathways of termination of the polymer chain.

size of the counterions, theoretical studies of the mechanisms of insertion and termination, with the counterion incorporated, are difficult and involve considerable computational effort. Hence, few examples of such studies are found in the literature. Nifant'ev et al.[8] have studied ethylene insertion for the $Cp_2ZrEt^+A^-$ (A^- = $CH_3B(C_6F_5)_3^-$, $B(C_6F_5)_4^-$) systems. Lanza et al.[9a] have investigated olefin insertion into the Ti−CH_3 bond of the $H_2Si(C_5H_4)(^tBuN)TiCH_3-CH_3B(C_6F_5)_3$ ion pair; Fusco[9b] and Bernardi[9c] studied the same process for $Cp_2(Ti/Zr)CH_3-Cl_2Al[OAl(CH_3)_3AlHCH_3]_2$ and $Cl_2TiCH_3(\mu\text{-}Cl)_2AlH_2$, respectively. Chan et al.[9d] have investigated the formation of ethylene-separated ion-pair complexes for ion pairs formed between different catalysts and the counterion $B(C_6F_5)_3CH_3^-$, as well as ethylene insertion[9i] into the Zr−C_2H_5 bond in the $Cp_2Zr-C_2H_5-\mu\text{-}CH_3\text{-}B(C_6F_5)_3$ system.

In earlier theoretical studies, we have investigated the insertion and termination (by β hydrogen transfer to monomer) processes for the system $[Cp\{NC(^tBu)_2\}\text{-}TiR\text{-}\mu\text{-}CH_3\text{-}B(C_6F_5)_3]$[10a] (R = Me, Pr) and the PI system $[(C_6H_5N{=}CH)C_4H_3N]_2\text{-}Pr\text{-}\mu\text{-}CH_3\text{-}B(C_6F_5)_3$,[10b] incorporating counterion and solvent effects. A validated[10c] QM/

(6) (a) Tsutsui, T.; Mizuno, A.; Kashiwa, N. *Polymer* **1989**, *30*, 428. (b) Stehling U.; Diebold, J.; Kirsten, R.; Roll, W.; Brintzinger, H.-H. *Organometallics* **1994**, *13*, 964. (c) Resconi, L.; Piemontesi, F.; Camurati, I.; Balboni, D., Sironi, A.; Moret, M.; Rychlicki, H.; Ziegler, R. *Organometallics* **1996**, *15*, 5046. (d) Lehmus, P.; Kokko, E.; Harkki, O.; Leino, R.; Luttikhedde, H. J. G.; Nasman, J. H.; Seppala, J. V. *Macromolecules* **1999**, *32*, 3547. (e) Lehmus, P.; Kokko, E.; Leino, R.; Luttikhedde, H. J. G.; Rieger, B.; Seppala, J. V. *Macromolecules* **2000**, *33*, 8534. (f) Voegele, J.; Troll, C.; Rieger, B. *Macromol. Chem. Phys.* **2002**, *203*, 1918. (g) Chen, M.-C.; Roberts, J. A. S.; Marks, T. J. *J. Am. Chem. Soc.* **2004** *126*, 4605.

(7) (a) Woo, T. K.; Margl, P. M.; Ziegler, T.; Blöchl, P. E. *Organometallics* **1997**, *16*, 3454. (b) Woo, T. K.; Margl, P. M.; Lohrenz, J. C. W.; Blöchl, P. E.; Ziegler, T. *J. Am. Chem. Soc.* **1996**, *118*, 13021. (c) Margl, P. M.; Lohrenz, J. C. W.; Blöchl, P. E.; Ziegler, T. *J. Am. Chem. Soc.* **1996**, *118*, 4434. (d) Deng, L.; Woo, T. K.; Cavallo, L.; Margl, P. M.; Ziegler, T. *J. Am. Chem. Soc.* **1997**, *119*, 6177.

(8) Nifant'ev, I. E.; Ustynyuk, L. Y.; Laikov, D. N. *Organometallics* **2001**, *20*, 5375.

(9) (a) Lanza, G.; Fragala, I. L.; Marks, T. J. *Organometallics* **2002**, *21*, 5594. (b) Fusco, R.; Longo, L.; Masi, F.; Garbassi, F. *Macromol. Rapid Commun.* **1998**, *19*, 257. (c) Bernardi, F.; Bottoni, A.; Miscione, G. P. *Organometallics* **1998**, *17*, 16. (d) Chan, M. S. W.; Vanka, K.; Pye, C. C.; Ziegler, T. *Organometallics* **1999**, *18*, 4624. (e) Vanka, K.; Ziegler, T. *Organometallics* **2001**, *20*, 905. (f) Zurek, E.; Woo, T. K.; Firman, T.; Ziegler, T. *Inorg. Chem.* **2001**, *40*, 361. (g) Zurek, E.; Ziegler, T. *Inorg. Chem.* **2001**, *40*, 3279. (h) Zurek, E.; Ziegler, T. *Organometallics*, in press. (i) Chan, M. S. W.; Ziegler, T. *Organometallics* **2000**, *19*, 5182.

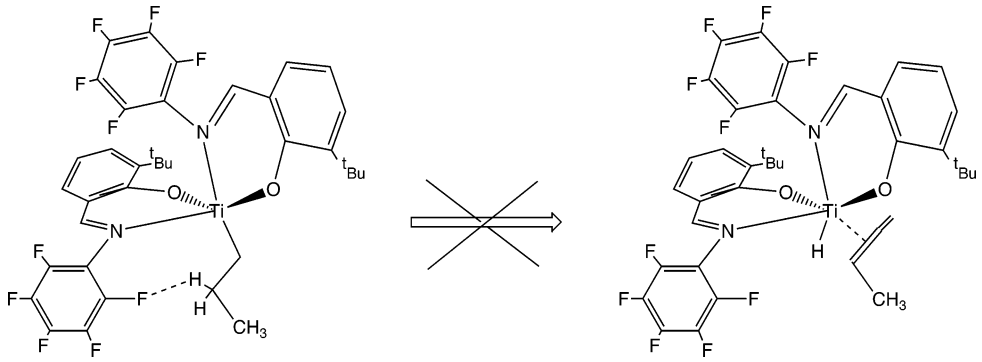

Figure 5. Ortho-fluorine effect.

MM model was employed to model the counterion, $B(C_6F_5)_3CH_3^-$, in these studies. The current investigation focuses again on the PI system. Mitani et al.[4e] found that the titanium-based phenoxy−imine (FI) systems showed features of living polymerization upon substitution of a hydrogen by fluorine in the ortho position of the phenyl group attached to the chelating nitrogen. They explained this "ortho-fluorine" effect by assuming an interaction between the ortho fluorine and the β-hydrogen of the chain. This would inhibit the β -hydrogen transfer to the metal, which they considered the principal mode of chain termination (see Figure 5).

Interestingly, Reinartz et al.[4f] have also studied the FI catalyst system experimentally and found it to be living in the *absence* of ortho fluorines on the aryl ring attached to the nitrogen. They conclude in their paper that "factors (other than the ortho-fluorine effect) could be involved in determining the relative rates of propagation and chain transfer". It is clear, therefore, that the question of why some of the post-metallocene systems exhibit living polymerization behavior has not been fully resolved yet.

In the current study, we aim to address this issue by analyzing the ortho-fluorine effect. This will be done by studying two PI systems, $[(C_6R_5N{=}CH)C_4H_3N]_2PrTi$-$\mu$-$CH_3$-$B(C_6F_5)_3$ (R = F, H). (It is true that the ortho-fluorine effect has been experimentally tested for the FI systems, but the PI systems are structurally very similar to the FI systems. Moreover, a slightly modified version of the PI systems, the indolide−imine system[13] (see Figures 1 and 2) have exhibited living polymerization behavior.) The objective is to determine how altering "R" (F or H) in the aryl ring attached to the imine nitrogen affects the two (uni- and bimolecular) chain termination processes. The entire cationic system will be treated as full QM, with only the counterion $B(C_6F_5)_3CH_3^-$ being modeled with QM/MM, using the validated model mentioned earlier. The configuration of the PI systems that will be considered is the one that has been experimentally obtained[4b] by X-ray crystallographic analyses of several different PI catalyst systems. The effect of the solvent on the insertion process will also be considered, with single-point solvation calculations carried out to determine the energy of solvation for the ion pair, the olefin complexes, and the transition states. Cyclohexane ($\epsilon = 2.023$) will be used as the solvent. We will also compare and contrast the results obtained for the two PI systems by obtaining ethylene insertion and termination barriers for the indenyl system [bis(η^5-1-indenyl)dimethylsilane)]ZrPr-μ-Me-$B(C_6F_5)_3$ (which has been experimentally studied[6f]) and also by studying the effect of increasing the steric bulk on the aryl groups attached to the imine nitrogens on the termination process.

II. Computational Details

The density functional theory calculations were carried out using the Amsterdam Density Functional (ADF) program version 2000.01, developed by Baerends et al.[11] and vectorized by Ravenek.[12] The numerical integration scheme applied was developed by te Velde et al.,[13] and the geometry optimization procedure was based on the method of Verslius and Ziegler.[14] Geometry optimizations were carried out using the local exchange-correlation potential of Vosko et al.[15] without any symmetry constraints. The electronic configurations of the atoms were described by a triple-ζ basis set on titanium (n = 3) and zirconium (n = 4) for ns, np, nd, and (n + 1)s, augmented with a single (n + 1)p polarization function. Double-ζ STO basis sets were used for carbon (2s, 2p), hydrogen (1s), and nitrogen (2s, 2p), augmented with a single 3d polarization function, except for hydrogen, where a 2p polarization function was used. Shells of lower energy were treated by the frozen-core approximation. A set of auxiliary s, p, d, f, and g STO functions centered on all nuclei was used to fit the molecular density and represent Coulomb and exchange potentials accurately in each SCF cycle.[16] The gas-phase energy difference was calculated by augmenting the local density approximation energy with Perdew and Wang's non-local correlation and exchange corrections (PWB91).[17] The solvation energies were obtained from a single-point full QM calculation using the conductor-like screening model (COSMO)[18] and optimized geometries from QM/MM calculations.

(10) (a). Vanka, K.; Xu, Z.; Ziegler, T. *Can. J. Chem.* **2003**, *81*, 1413. (b) Vanka, K.; Xu, Z.; Ziegler, T. *Organometallics* **2004**, *23*, 2900. (c) Xu, Z.; Vanka, K.; Firman. T.; Michalak, A.; Zurek, E.; Zhu, C.; Ziegler, T. *Organometallics* **2002**, *21*, 2444. (d) Vanka, K.; Xu, Z.; Ziegler, T. *Isr. J. Chem.* **2002**, *42* (4), 403. (e) Zurek, E.; Ziegler, T. *Faraday Discuss.* **2003**, *124*, 93. (f) Xu, Z.; Vanka, K.; Ziegler, T. *Organometallics* **2004**, *23*, 104.

(11) (a) Baerends, E. J.; Ellis, D. E.; Ros, P. *Chem. Phys.* **1973**, *2*, 41. (b) Baerends, E. J.; Ros, P. *Chem. Phys.* **1973**, *2*, 52. (c) te Velde, G.; Baerends, E. J. *J. Comput. Phys.* **1992**, *92*, 84. (d) Fonseca, C. G.; Visser, O.; Snijders, J. G.; te Velde, G.; Baerends, E. J. In *Methods and Techniques in Computational Chemistry, METECC-95*; Clementi, E., Corongiu, G., Eds.; STEF: Cagliari, Italy, 1995; p 305.

(12) Ravenek, W. In *Algorithms and Applications on Vector and Parallel Computers*; te Riele, H. J. J., Dekker, T. J., van de Horst, H. A., Eds.; Elservier: Amsterdam, The Netherlands, 1987.

(13) (a) te Velde, G.; Baerends, E. J. *J. Comput. Chem.* **1992**, *99*, 84. (b) Boerrigter, P. M.; te Velde, G.; Baerends, E. J. *Int. J. Quantum Chem.* **1998**, *33*, 87.

(14) Verslius, L.; Ziegler, T. *J. Chem. Phys.* **1988**, *88*, 322.

(15) Vosko, S. H.; Wilk, L.; Nusair, M. *Can. J. Phys.* **1980**, *58*, 1200.

(16) Krijn, J.; Baerends, E. J. *Fit Functions in the HFS-Method*; Free University of Amsterdam, Amsterdam, 1984.

(17) Perdew, J. P. *Phys. Rev. B* **1992**, *46*, 6671.

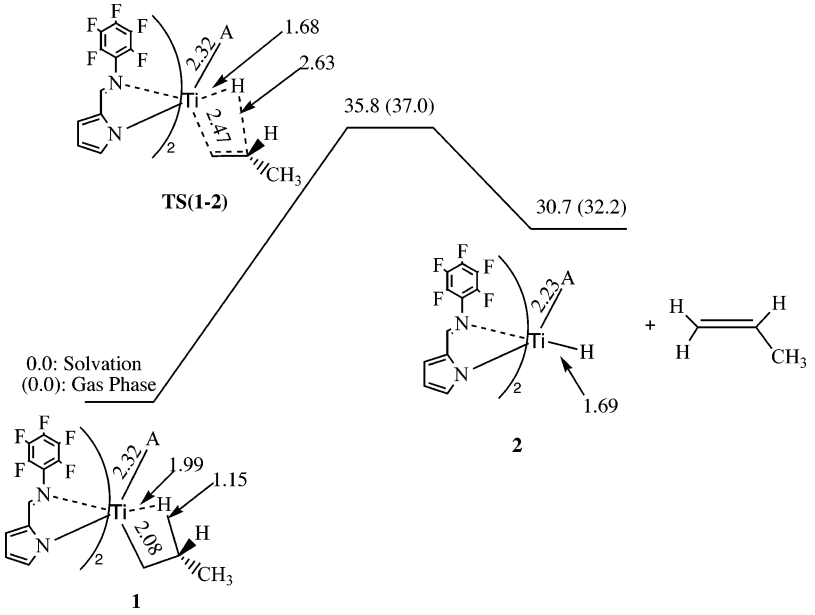

Figure 6. Energy profile for unimolecular termination, for the fluorine case.

A dielectric constant of 2.023 was used to represent cyclohexane as the solvent. The radii used for the atoms (in Å) were as follows: C, 2.0; H, 1.16; B, 1.15; N, 1.5; F, 1.2; Ti, 2.3; Cl, 2.1. Only the electronic contribution was calculated to evaluate the enthalpy of the reactions considered in this work. The enthalpies (ΔH) reported in the following sections are potential energy differences without zero-point corrections or vibrational finite temperature corrections. Such corrections are still too expensive to calculate for the size of molecules considered here. We expect these corrections to be of the order of ±2−3 kcal/mol. The insertion barriers were obtained by doing linear transit calculations for the same reaction coordinates, the C−C distance between one C of the ethylene and the C_α of the CH_3 or C_3H_7 groups, which represent the growing chains. The MM atoms were described using the SYBYL/TRIPOS 5.2 force field constants.[19a] The code for QM/MM in ADF has been implemented by Woo et al.[19b]

III. Results and Discussion

a. (i) Termination by *β*-Hydrogen Transfer to Metal: "Fluorine Case". The unimolecular termination process of transfer of hydrogen from the β−carbon of the chain to the titanium metal center (see Figure 4) was investigated first, for the system $[(C_6F_5N{=}CH)\text{-}C_4H_3N]_2PrTi\text{-}\mu\text{-}CH_3\text{-}B(C_6F_5)_3$, i.e., with fluorines attached to the phenyl group on the imine nitrogen— the "fluorine case". The energy profile for the termination is shown in Figure 6. An agostic interaction exists in the contact ion pair, **1**, between a hydrogen on the β-carbon and the metal center. As the hydrogen is extracted from the carbon, R(H−C) increases from 1.15 Å (in the contact ion pair) to 2.63 Å in the transition state, **TS(1-2)** (see Figure 6). R(Ti−H), meanwhile, has decreased from 1.99 Å to 1.68 Å. The counterion (A in the figure) is not displaced at all during this transfer. However, the distance between the α-carbon of the chain and the titanium metal center increases, from 2.08 Å in **1** to 2.47 Å in **TS(1-2)**. This loss of bonding, coupled with the loss of bonding of the β-carbon with the hydrogen, leads to a rise in energy, from 0.0 kcal/mol in **1** to 35.8 kcal/mol in **TS(1-2)** (see Figure 6).

After the transition state is crossed, the system starts to stabilize, with the chain detaching from the metal center as a substituted ethylene. Finally, at complete separation of the substituted ethylene, the titanium hydride complex **2** is formed, 30.7 kcal/mol above the reactant species **1** (see Figure 6).

Since the counterion is not displaced at all during this transfer process, solvent effects are marginal, as there is little or no charge separation in the system on going from **1** to **2**. The gas-phase energies (indicated in parentheses) are only slightly higher than the solvent-corrected energies. Therefore, overall, the numbers indicate that the process of β-hydrogen transfer to the metal is a highly endothermic process, and the product formed from the transfer (**2**) also lies substantially above the stable contact ion pair (**1**) on the potential energy surface.

(ii) Rearrangement Reaction: Transfer of Cocatalyst, $B(C_6F_5)_3$, from Carbon to Hydrogen. The product **2**, formed from the transfer of hydrogen from the β-carbon to the metal and discussed above, has the cocatalyst $B(C_6F_5)_3$ attached to the bridging methide group that is, in turn, connected to the titanium metal center. In the presence of two methyl groups attached to the titanium, this methide-bridged ion pair is typically formed. However, in a complex such as **2**, with a hydrogen and a methyl attached to the titanium, it might be possible for the cocatalyst to rearrange by detaching itself from the methyl group and reattaching to the hydrogen, to form a hydrogen-bridged complex. Landis et al.[20] have found experimental evidence of such a complex for their *ansa*-indenyl system. We investigated the energetics of such a rearrangement for **2**. Figure 7 shows the energy profile for the transfer of the cocatalyst from the methyl group to the hydrogen.

The transfer occurs by a dissociative process, during which the boron loses its bonding to the bridging carbon,

(18) (a) Klamt, A.; Schuurmann, G. *J. Chem. Soc., Perkin Trans. 2* **1993**, 799. (b) Pye, C. C.; Ziegler, T. *Theor. Chem. Acc.* **1999**, *101*, 396.

(19) (a) Clark, M.; Cramer, R. D., III; van Opdenbosch, N. *J. Comput. Chem.* **1989**, *10*, 982. (b) Woo, T. K.; Cavallo, L.; Ziegler, T. *Theor. Chim. Acta* **1998**, *100*, 307. (c) Maseras, F.; Morokuma, K. *J. Comput. Chem.* **1995**, *16*, 1170.

(20) Sillars, D. R.; Landis, D. R. *J. Am. Chem. Soc.* **2003**, *125*, 9894.

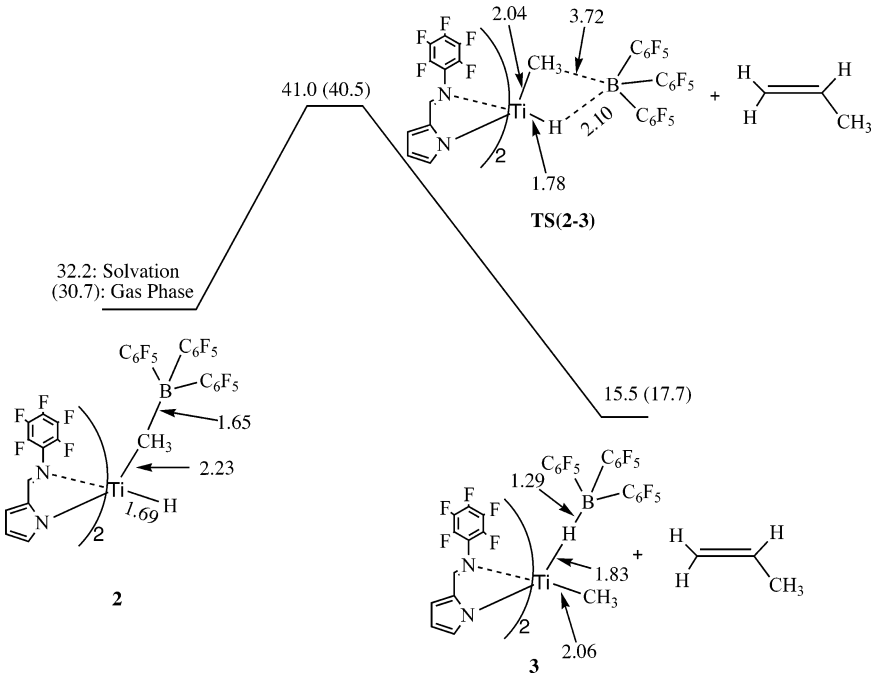

Figure 7. Reorganization of the methyl-bridged contact ion pair to the hydrogen-bridged contact ion pair.

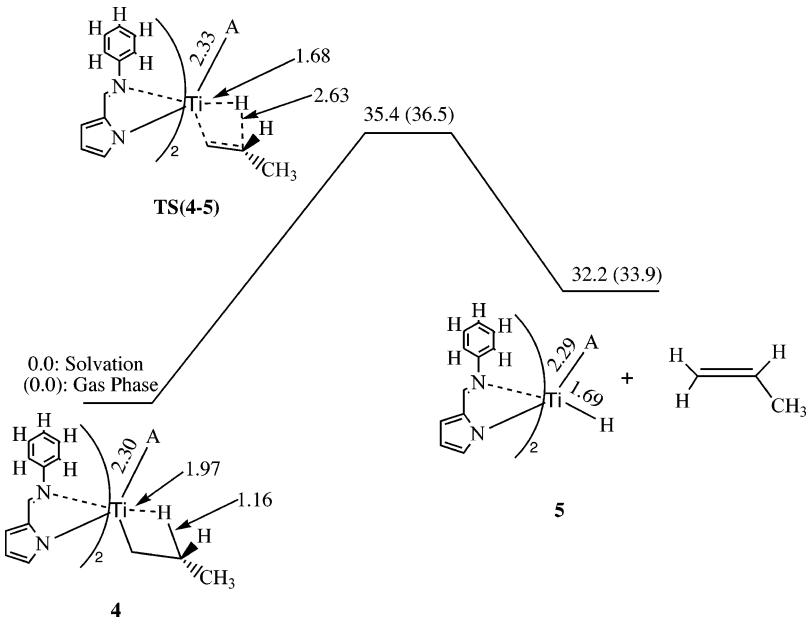

Figure 8. Energy profile for unimolecular termination, for the hydrogen case.

in going from **2** to the transition state **TS(2-3)**. R(B−C) increases from 1.65 Å in **2** to 3.72 Å in **TS(2-3)** (see Figure 7). Moreover, at this point, the boron, having moved away from the carbon, has begun to approach and bond with the hydrogen and is 2.10 Å from it. This dissociation of the cocatalyst from the carbon is understandable, because the σ-orbital on the boron has to reorient itself away from the carbon and toward the hydrogen, to form a new bond, and this necessitates the displacement of the cocatalyst. This also leads to a rise in energy by 8.8 kcal/mol with reference to **2**. Therefore, since **2** lies 32.2 kcal/mol above the original contact ion pair, **1**, **TS(2-3)** lies 41.0 kcal/mol above **1** on the potential energy surface (see Figure 7).

After the transition state is crossed, the boron continues to approach the hydrogen, until R(B−H) is 1.29 Å and the new hydrogen-bridged contact ion pair **3** has been formed (see Figure 8). This lies 15.5 kcal/mol above **1**; i.e., it is 16.7 kcal/mol more stable than **2** (32.2 kcal/mol above **1**) (see Figure 7). This suggests that, if complex **2** is allowed to remain in the absence of monomer for a long time, it might eventually prefer to rearrange itself to form **3**. In the presence of monomer, such a rearrangement would be unlikely, because the monomer would insert into the Ti−H bond in **2**, and so the hydrogen-bridged complex would never be formed. This would explain the experimental evidence for the hydrogen-bridged complex when free monomer was excluded from the reaction chamber.[20]

(iii) Termination by β-Hydrogen Transfer to Metal: "Hydrogen Case". Termination by transfer from the β-carbon of the chain to the metal center had been discussed earlier in section IIIa(i) for the "fluorine case", i.e., the $[(C_6F_5N{=}CH)C_4H_3N]_2PrTi$-$\mu$-$CH_3$-$B(C_6F_5)_3$

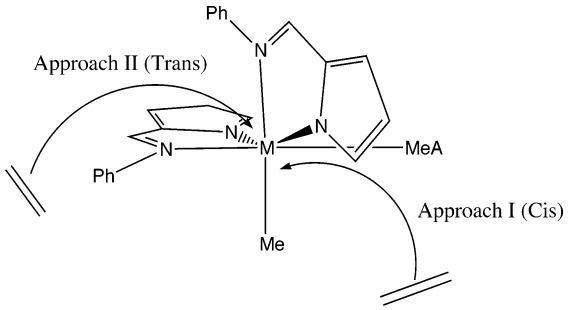

Figure 9. Different modes of approach of the ethylene monomer toward the octahedral contact ion pair.

system. The termination process for the system $[(C_6H_5N{=}CH)C_4H_3N]_2RTi\text{-}\mu\text{-}CH_3\text{-}B(C_6F_5)_3$—i.e., with hydrogens in the phenyl group attached to the imine nitrogen or the "Hydrogen Case"—was studied next. This was done to determine whether there really was an ortho-fluorine effect that led to the fluorine case having a higher termination barrier than the hydrogen case (as mentioned in the Introduction). Figure 8 shows the energy profile for the hydride transfer. As in the fluorine case, an agostic interaction exists between a hydrogen on the β-carbon of the chain and the metal center in the contact ion pair **4**. The transition state **TS(4-5)** is also similar to **TS(1-2)** in that (i) the counterion A is not displaced from the metal center, (ii) the α-carbon of the chain is displaced to about the same amount, from 2.08 Å in **4** to 2.47 Å in **TS(4-5)**, and, most importantly, (iii) the rise in energy in going from **4** to **TS(4-5)**, 35.4 kcal/mol, is nearly the same as that for the fluorine case (35.8 kcal/mol) (see Figure 8). What this suggests is that altering the catalyst by having hydrogens instead of fluorines in the ancillary phenyl group does not lead to a significant decrease in the termination barrier; i.e., the ortho fluorine does not appear to influence the height of the termination barrier.

After the transition state is crossed, the system proceeds toward the formation of the hydrido complex **5**, analogous to complex **2** for the fluorine case. This lies 32.2 kcal/mol higher than the reactant, **4**, on the potential energy surface (see Figure 8).

b. Investigating the Bimolecular Pathway for Chain Termination. The barriers for the process of the unimolecular β-hydrogen transfer to the metal, studied for the two cases, are substantially high, at about 36 kcal/mol. Mitani et al.[4e] had assumed this to be the principal pathway of chain termination, but given the height of the barriers, it is clear that the alternate termination process possible for these systems, the bimolecular transfer of a hydrogen from the β-carbon of the chain to the monomer (see Figure 4), has to be investigated for the two systems. The next two subsections focus on this pathway of chain termination.

It was determined from previous calculations[10] that two approaches of the monomer toward the metal center can lead to π-complexation and subsequent insertion or termination. As shown in Figure 9, the monomer (ethylene in this case) can approach cis to the methyl bridge between the metal and the cocatalyst—the "cis" approach—or attempt an approach that is nearly trans to the methyl bridge—the "trans" approach. Previous calculations with the PI system[10b] showed that the monomer approach which led to the most facile bimolecular chain termination was (i) when the ethylene approached cis to the methyl bridge and (ii) when the propyl chain attached to the metal was oriented so that the dihedral angle formed between the β-carbon, α-carbon, and titanium metal center and the α-carbon, titanium, and the μ-methyl carbon was close to 0°—the "0° orientation". The bimolecular chain termination process, discussed in the next two subsections for the PI system, will therefore be studied for this most favorable case: cis approach of the ethylene with the propyl chain in the 0° orientation.

(i) β-Hydrogen Transfer to the Monomer: Fluorine Case. Figure 10 shows the energy profile for the transfer of β-hydrogen to the ethylene monomer, for the fluorine case. The contact ion pair $[(C_6F_5N{=}CH)C_4H_3N]_2PrTi\text{-}\mu\text{-}CH_3\text{-}B(C_6F_5)_3$ (**6**) lies 2.3 kcal/mol above the most stable confomer for the contact ion pair **1**, discussed earlier with reference to β-hydrogen transfer to the metal.

To form the π complex, the ethylene monomer has to approach **6**, and this necessitates the displacement of the counterion from the metal center so that room can be made to accommodate the ethylene moiety. This leads to a rise in energy for the system, until **TS(6-7)** is reached on the potential energy surface. This represents the transition state to uptake for the monomer, prior to formation of the π-complex with the metal center. At this point, the counterion A has been displaced from the metal center from 2.46 Å (in **6**) to 3.51 Å, while the ethylene is now 3.00 Å away from the metal center. The agostic interaction between the hydrogen and the metal center is still preserved at this point, though R(Ti−H) has increased slightly from 1.99 to 2.23 Å. The displacement of the counterion and the increased steric crowding due to the approach of the ethylene monomer leads to a rise in energy for the system, to 17.2 kcal/mol (see Figure 10). This is the barrier for monomer uptake for the system.

As the ethylene continues to approach and complex to the metal center, the energy drops and eventually the π-complex **7** is formed, lying 4.1 kcal/mol above **6** on the potential energy surface. By this point, the counterion has been displaced to 5.27 Å away from the metal center, and the ethylene lies 2.43 Å away from the titanium (see Figure 10). The metal center finds some stabilization for the loss of bonding to the counterion from the strengthening of the β-agostic interaction between hydrogen and titanium, with R(Ti−H) reduced to 1.95 Å in **7** in comparison to 2.23 Å in **6** (see Figure 10).

Following the π-complexation, one of the carbons of the ethylene begins to bond to the metal center, while the other approaches and begins to extract the hydrogen that is weakly bonded to the metal. (The chain, at this point, could rotate out of the plane containing the metal center, the α- and β-carbons, and the agostic hydrogen, to allow insertion to take place, but this rotation has been found in earlier studies[10b] to have a prohibitively high barrier.) This results in a rise in energy, leading eventually to the formation of the transition state **TS(7-8)** (see Figure 10). At this stage, one of the carbons of the ethylene is bonded to the titanium, at a distance of 2.22 Å, while the other lies 1.45 Å from the hydrogen, part of the six-membered transition state for the hydride transfer. The hydride transfer barrier is 9.2 kcal/mol

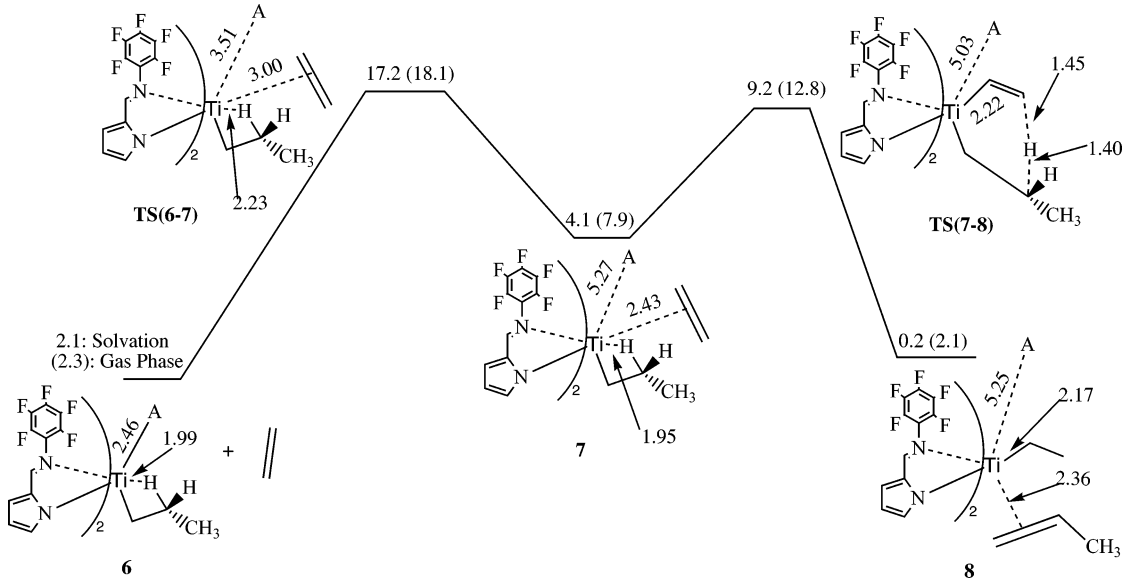

Figure 10. Energy profile for bimolecular termination, for the fluorine case.

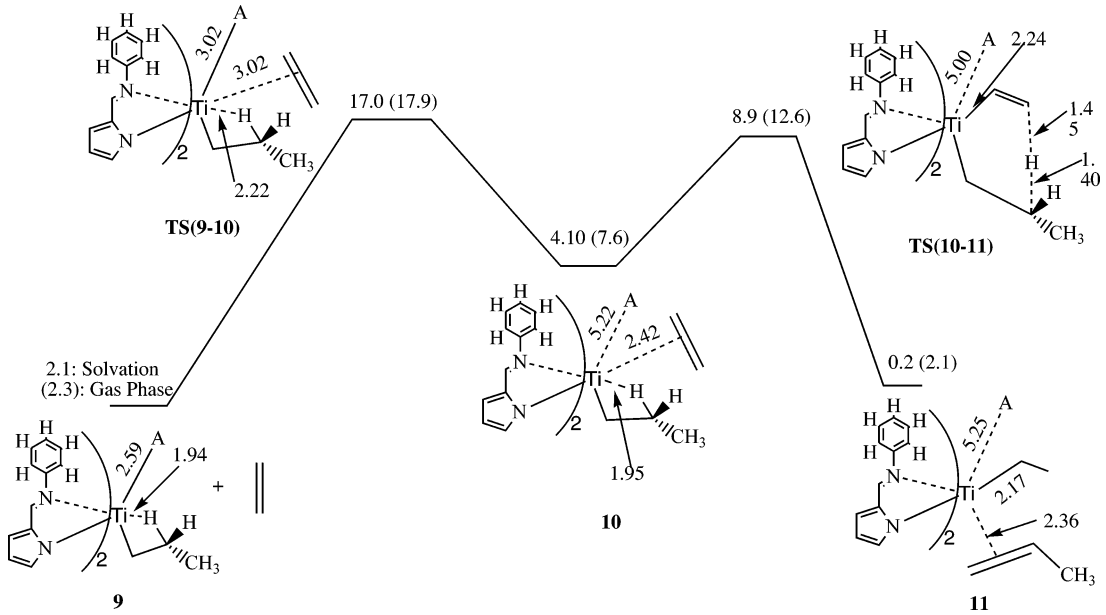

Figure 11. Energy profile for bimolecular termination, for the hydrogen case.

(see Figure 10), which is lower than the uptake barrier (17.2 kcal/mol). Hence, the uptake is the rate-determining step for the transfer process.

After crossing the hydride transfer transition state, the system goes downhill in energy, until **8** is formed, which is only slightly less stable than **6** (0.2 kcal/mol) on the potential energy surface. The complex at this point has an ethyl chain attached to the titanium, while the erstwhile propyl chain, after loss of the hydrogen, is now a substituted ethylene moiety and forms a π-complex to the metal center. The counterion A is still distant from the metal center, lying 5.25 Å away from the titanium.

The rate-determining barrier to this chain termination process for the $[(C_6F_5N{=}CH)C_4H_3N]_2PrTi\text{-}\mu\text{-}CH_3\text{-}B(C_6F_5)_3$ system is therefore the uptake barrier of 17.2 kcal/mol. On the potential energy surface, this is 18.6 kcal/mol lower than the barrier for the other chain termination process: hydrogen transfer to the metal center. Entropic effects have not been considered in the studies, and it is true that they would affect the bimolecular termination by hydrogen to monomer more adversely than the unimolecular hydrogen transfer to the metal center. However, one would estimate, at most, an entropic contribution of 15 kcal/mol to the barrier, and even making such an allowance and increasing the bimolecular barriers by that amount, it would appear that the β-hydrogen transfer to the monomer would still be the preferred route to termination of the chain.

(ii) β-Hydrogen Transfer to the Monomer: Hydrogen Case. Figure 11 shows the energy profile for the transfer of the β-hydrogen to the ethylene monomer for the $[(C_6H_5N{=}CH)C_4H_3N]_2PrTi\text{-}\mu\text{-}CH_3\text{-}B(C_6F_5)_3$ system: i.e., the "hydrogen case". The ethylene approaches the conformer **9** (see Figure 11). **9** has a propyl chain in the 0° orientation and lies 2.1 kcal/mol above the most stable conformer **4** (see Figure 6). As in the "fluorine case", an uptake transition state, **TS(9-10)**, is reached on the potential energy surface before the ethylene can form a π-complex with the metal center. The principal

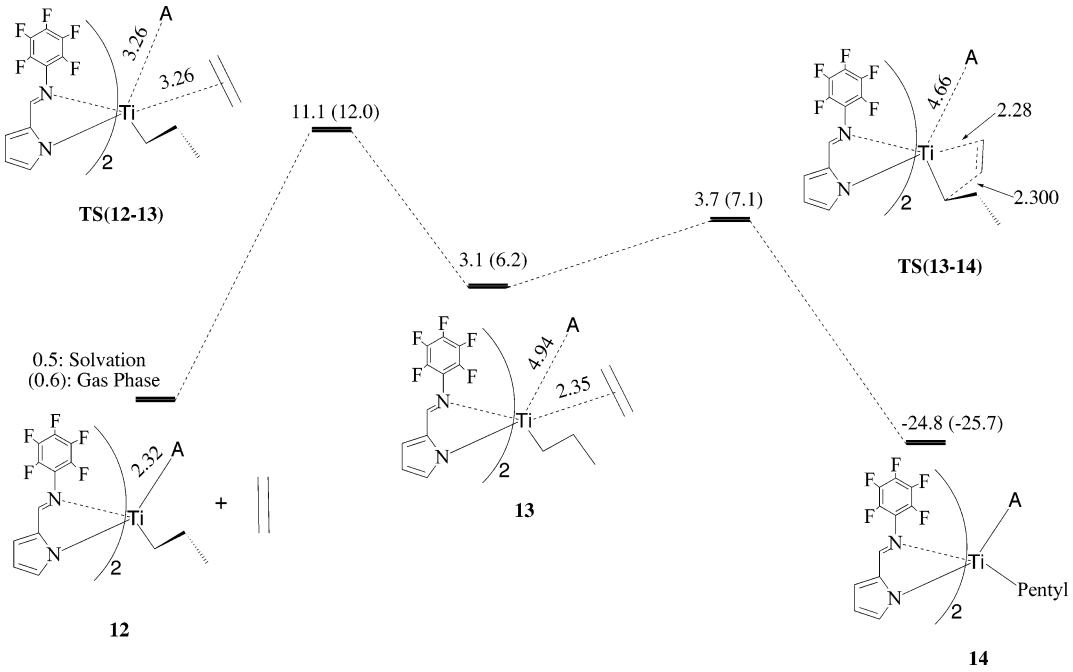

Figure 12. Energy profile for the most favorable insertion pathway, for the fluorine case.

features of this transition state, viz. displacement of the counterion (R(Ti−μ-C) increases from 2.59 to 3.02 Å), the weakening of the β agostic interaction of the β-hydrogen with the titanium (R(Ti-H) increases from 1.94 to 2.22 Å), and the distance of the ethylene from the metal center (3.00 Å) are all similar for the corresponding fluorine case (see Figures 10 and 11). The uptake barriers are also found to be close: 17.0 kcal/mol for the hydrogen case as opposed to 17.2 kcal/mol for the fluorine case.

After the uptake transition state is crossed, the π-complex **10** is formed, lying 4.1 kcal/mol above **9**. As in the π-complex **6**, in the fluorine case, the counterion in **10** is considerably displaced (R(Ti−A) = 5.22 Å), the agostic interaction between the β-hydrogen and the metal is strengthened (R(Ti−H) decreases from 2.22 Å in **TS(9-10)** to 1.95 Å in **10**), and the ethylene monomer lies 2.42 Å away from the metal center (see Figure 11).

Likewise, in the principal geometric features, the hydrogen transfer transition state **TS(10-11)** is a carbon copy of the corresponding hydrogen transfer transition state for the fluorine case, **TS(6-7)**. The counterion remains displaced (R(Ti−A) = 5.00 Å), one of the carbons of the ethylene forms a bond to the titanium (R(Ti−C) = 2.24 Å), and the other approaches the β-hydrogen (R(C−H) = 1.45 Å). The barrier to the hydride transfer, 8.9 kcal/mol, is only slightly lower than the corresponding barrier for the fluorine case of 9.2 kcal/mol (see Figure 12). The product that is subsequently formed, **11**, is, again in all respects similar to the corresponding product **7** for the fluorine case.

The similarity in the geometric features and the energy values between the corresponding complexes along the reaction path for the fluorine and hydrogen cases of the PI system is a further indication that the substitution of fluorines for hydrogens in the phenyl ring does not have an effect on the polymerization process. In other words, the ortho-fluorine effect proposed[4e] and mentioned in the Introduction does not seem to be present in the PI system. It is possible that the stability of the catalyst is improved by having an ortho fluorine on the phenyl ring, since catalyst deactivating reactions that would otherwise occur, such as extraction of an ortho hydrogen on the phenyl ring attached to the imine nitrogen, would be impeded by the substitution of the ortho hydrogen by a fluorine. This may explain the ortho-fluorine effect. On the other hand, it is also possible that the ortho-fluorine effect may not be the principal reason for the living polymerization at all, as noted by Reinartz et al.[4f] Our calculations would certainly seem to corroborate this view.

c. Most Favorable Pathway for Insertion for [(C_6R_5N=CH)C_4H_3N]$_2$PrTi-μ-CH_3-B(C_6F_5)$_3$ (R = F, H). To complete the picture, we also decided to look at the most favorable pathway for insertion for the hydrogen and fluorine cases. Earlier investigations on the PI system[10b] had shown that the cis approach of the ethylene monomer when the chain was in a +80° orientation (i.e. when the the plane containing the β-carbon of the chain, α-carbon of the chain, and the metal center made a dihedral angle of +80° with the plane containing the α-carbon, the metal center, and the μ-methyl carbon) led to the lowest barriers to insertion. Figures 12 and 13 show the respective energy profiles for the insertion. Beginning with the approach of the ethylene toward the conformers **12** and **15**, respectively (lying 0.5 kcal/mol above the most stable conformers **1** and **4**), that have θ equal to 80°, the uptake transition states **TS(12-13)** and **TS(15-16)**, respectively, were encountered for the two cases before π-complexation occurred. The features are the same in **TS(12-13)** and **TS(15-16)**: (i) moderate displacement of the counterion (from 2.32 Å in the contact ion-pairs to 3.26 Å in **TS(12-13)** and 3.16 Å in **TS(15-16)**), (ii) similar distance of the ethylene π-complex from the metal center (3.26 in **TS(12-13)** and 3.32 Å in **TS(15-16)**), and (iii) barriers of 11.1 kcal/mol for **TS(12-13)** and 11.2 kcal/mol for **TS(15-16)** (see Figures 12 and 13).

The π-complexes **13** and **16**, respectively, which are subsequently formed after ethylene uptake, have the

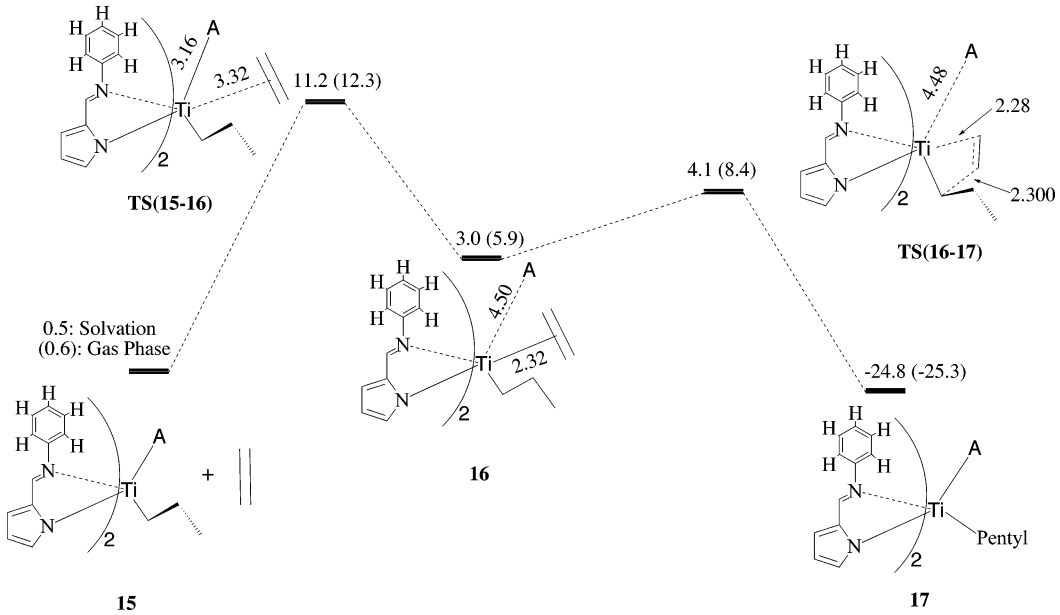

Figure 13. Energy profile for the most favorable insertion pathway, for the hydrogen case.

counterion displaced from the vicinity of the metal center (*R*(Ti−A): 4.94 Å in **13** and 4.50 Å in **16**) and have the ethylene at a distance of about 2.35 Å from the titanium. The complexes lie 3.1 kcal/mol above the reactant contact ion pairs on the energy surface (see Figures 12 and 13).

After π-complex formation, one of the carbons on the ethylene begins to bind to the metal center, while the other approaches the α-carbon of the chain. This leads to a rise in energy and, eventually, to the formation of the transition state of insertion. In Figures 12 and 13, these are represented by **TS(13-14)** and **TS(16-17)** for the fluorine and hydrogen cases, respectively. In either transition state, the counterion remains displaced (*R*(Ti−A): 4.66 Å in **13** and 4.48 Å in **16**), the distance between the metal center and the bonding ethylene carbon is 2.28 Å, and the distance between the other ethylene and the α-carbon is 2.30 Å.

The barrier for the insertion is slightly greater for the hydrogen case, 4.1 kcal/mol, than the fluorine case, 3.7 kcal/mol.

With further approach of the ethylene carbon toward the α-carbon, the energy of the system decreases as bonding occurs, leading eventually to the formation of the products **14** and **17** for the respective cases (see Figures 12 and 13), lying about 25 kcal/mol below the respective reactants **12** and **15** on the potential energy surface.

The rate-determining uptake barriers for insertion for the two systems are about 6 kcal/mol lower in energy in comparison to the rate-determining uptake barriers for bimolecular chain termination, which agrees with previous calculations[10b] done on the PI systems.

As in the previous investigations of the termination processes, there is very little difference in the geometries or in the energy profiles for insertion between the fluorine and hydrogen Cases. All the calculations done suggest that both of the catalyst systems would behave in an identical fashion.

d. Increasing Steric Bulk on the Phenyl Group. It is known, from previous theoretical calculations on Brookhart type Ni(II) diimine systems,[7d] that the termination barrier increases more than the insertion barrier with an increase of steric bulk around the metal center, due to the greater steric requirements of the six-centered transition state for hydrogen transfer to monomer (see Figure 4), in comparison to the four-centered transition state for the insertion (see Figure 3). The theoretical calculations on the Brookhart systems, mentioned above,[7d] however, did not incorporate the counterion, and so the uptake barrier prior to both insertion and termination was not calculated for those cases.

We decided to investigate the effect of increasing the steric bulk on the bimolecular termination uptake and hydrogen transfer barriers, for the $[(C_6H_5N{=}CH)C_4H_3N]_2$-RTi-$\mu$-$CH_3$-$B(C_6F_5)_3$] system. The hydrogens in the ortho position were replaced by *tert*-butyl groups, which were treated as MM atoms, with hydrogen used to cap the QM system. Figure 14 shows the energy profile for the termination. Beginning from the contact ion pair **18** in the 0° orientation, the approach of the ethylene monomer gave rise to the uptake transition state **TS(18-19)**. The uptake barrier of 17.6 kcal/mol is comparable to the corresponding uptake barrier for the hydrogen case without steric bulk. After π-complex formation, the hydrogen transfer transition state **TS(19-20)** was found to be endothermic by 11.0 kcal/mol. This is 2.1 kcal/mol higher than the corresponding hydride transfer transition state for the non-bulky system, which shows that the presence of the bulky groups does indeed affect the sterically demanding six-centered transition state. However, since the rate-determining step is at the uptake of the ethylene monomer, which is not much different from the nonbulky hydrogen case, the influence of the bulky groups on the bimolecular termination process cannot be considered significant.

The final product, **20**, was determined to lie 0.2 kcal/mol above the reactants **18** and ethylene.

e. Investigating Uptake, Insertion, and Termination Barriers for the Bis(indenyl) System. Chain termination processes were experimentally investigated for the system [bis(η^5-1-indenyl)dimethylsilane]$ZrCl_2$ by Rieger et al.[6f] The bimolecular β-hydrogen transfer to

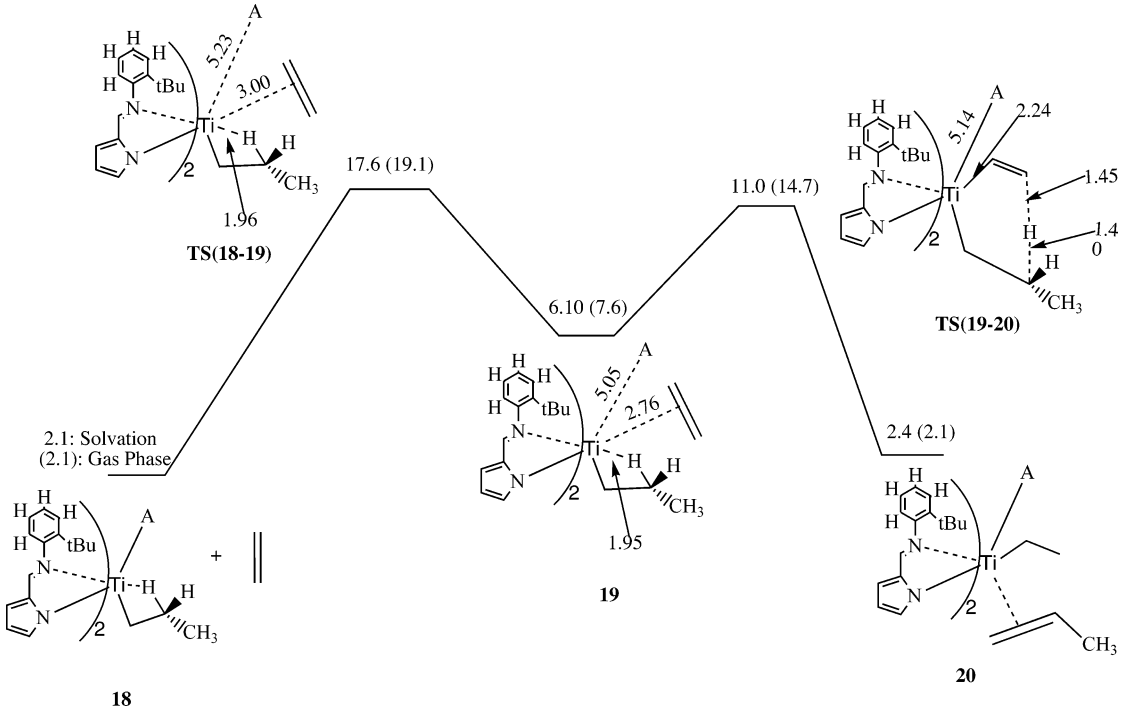

Figure 14. Energy profile for bimolecular termination, for the hydrogen case, with *tert*-butyl groups in the ortho positions of the phenyl rings attached to the imine nitrogens.

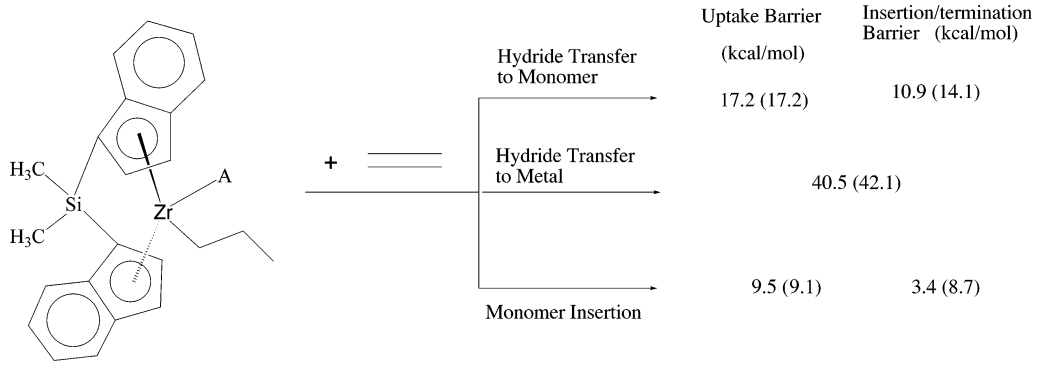

Figure 15. Insertion and termination barriers for the *ansa*-indenyl system.

the ethylene or propylene monomer was found to be the dominant termination process for this and analogous catalyst systems. Other, similar, *ansa*-indenyl zirconium systems[6] have been studied by other experimental groups, with similar conclusions being reached regarding the nature of the termination process. With our calculations regarding the termination in the pyrrolide–imide systems suggesting that this bimolecular termination would be favored (see sections IIIa and IIIb above), we decided to extend the investigation to [bis(η^5-1-indenyl)dimethylsilane]$ZrCl_2$, to determine if the calculations would corroborate the experimental findings for these systems. Figure 15 shows the results of the calculations done on the [bis(η^5-1-indenyl)dimethylsilane]ZrPr-μMe-B$(C_6F_5)_3$ system. The bimolecular β-hydrogen transfer to monomer, the unimolecular β-hydrogen transfer to metal, and the pathway leading to insertion for the ethylene monomer was studied for the ion-pair system. As was done for the PI system, discussed in the previous sections, only the most favorable approach of the ethylene was studied for the bimolecular insertion and termination processes.

The results for the insertion and termination by β-hydrogen transfer to monomer are similar to the values obtained for the PI system (see Figures 10–13), the values being close to the corresponding barriers for the PI system and other systems previously studied[10] to about 1–2 kcal/mol. This indicates that the nature of insertion and termination is similar across a wide range of different catalyst systems. It is interesting to note, though, that the barrier to the unimolecular β-hydrogen transfer to the metal is higher than the corresponding barrier for the PI system by about 5 kcal/mol (see Figure 15). This implies that the *ansa*-indenyl system would show a clear preference for bimolecular termination over unimolecular termination. This is in line with experimental findings[6] which show that the bis(η^5-1-indenyl)dimethylsilane)$ZrCl_2$ and analogous *ansa*-indenyl systems terminate by the bimolecular hydrogen transfer to the monomer, when $B(C_6F_5)_3$ is used as the activator.

IV. Conclusions

A density functional study was conducted to study two different chain termination processes for the two "PI" systems $[(C_6R_5N{=}CH)C_4H_3N]_2PrTi$-$\mu$-$CH_3$-$B(C_6F_5)_3$ (R = F, H): (i) unimolecular β-hydride transfer to the metal

center and (ii) bimolecular β-hydride transfer to the ethylene monomer. The counterion, $B(C_6F_5)_3CH_3^-$, was represented by a previously validated QM/MM model.[10c] The barriers for the bimolecular process were about 18 kcal/mol lower than the barrier for the unimolecular chain termination, indicating that the PI systems would prefer to terminate by hydride transfer to the incoming monomer, even if entropic effects were taken into account. Little or no difference was observed between the corresponding barriers for the two PI systems. This indicated that the experimentally observed "ortho-fluorine" effect in the similar FI catalyst systems was not significant in the PI case. This might also indicate that the living polymerization observed in the FI systems by Mitani et al.[4e] might be due to factors other than the ortho-fluorine effect, corroborating the experimental findings of Reinartz et al.[4f]

Insertion studies were also done for the two PI systems—the most favorable pathway (determined from earlier studies[10]) for insertion being investigated for each system and the uptake and insertion barriers calculated for each case. The difference between the rate-determining uptake barriers for insertion and the rate-determining uptake barriers for the bimolecular chain termination process for each of the two systems was about 6 kcal/mol. Again, there was little difference between the corresponding uptake and insertion barriers for the two PI systems. Both should produce polymers of high molecular weight in the absence of catalyst decomposition.

How the bimolecular termination process would be affected by the increase of steric bulk on the ancillary aryl rings was studied for the $[(C_6H_5N{=}CH)C_4H_3N]_2$-PrTi-$\mu$-$CH_3$-$B(C_6F_5)_3$ system, where the hydrogen in the ortho position of the aryl ring attached to the imine nitrogen was replaced by a *tert*-butyl group, modeled with MM atoms. The hydride transfer barrier increased, in comparison to the non-bulky PI system, by about 2 kcal/mol, but the rate-determining uptake barrier was not influenced as much, being only about 0.6 kcal/mol higher than the nonbulky hydrogen case.

Barriers for the most favorable insertion and termination (both uni- and bimolecular) were also calculated for the *ansa*-indenyl system [bis(η^5-1-indenyl)dimethylsilane]ZrPr-μMe-$B(C_6F_5)_3$. Barriers for the insertion and the bimolecular termination pathways were comparable to those for the PI system, as well as to the previously calculated systems,[10] indicating that the processes of insertion and termination for these different catalyst systems share common features. The barrier to the unimolecular termination by β-hydrogen transfer to the metal center was, however, found to be about 5 kcal/mol higher than for the PI systems and about 20 kcal/mol higher than the rate-determining uptake barrier to the bimolecular chain termination. This provides an explanation as to why a preference for bimolecular chain termination has been observed in experimental studies on *ansa*-indenyl systems,[6] when $B(C_6F_5)_3$ was used as an activator.

Acknowledgment. This investigation was supported by the Natural Science and Engineering Research council of Canada (NSERC) and by Mitsui Chemicals. T.Z. thanks the Canadian Government for a Canada Research Chair.

Supporting Information Available: Tables giving the optimized geometries of the structures reported (Cartesian coordinates, in Å). This material is available free of charge via the Internet at http://pubs.acs.org.

OM0492808